*Modeling the Dynamic Sensory Discharges of Insect Campaniform Sensilla

Nicholas S. Szczecinski[1][0000-0002-6453-6475], Sasha N. Zill[2][0000-0001-7472-8406], Chris J. Dallmann[3][0000-0002-4944-920X], and Roger D. Quinn[1][0000-0002-8504-7160]

[1] Case Western Reserve University, Cleveland, OH 44106, USA
[2] Marshall University, Huntington, WV 25755, USA
[3] University of Washington, Seattle, WA 98195, USA
nss36@case.edu

Abstract. Insects monitor the forces on their legs via sensory organs called campaniform sensilla (CS) that detect cuticular strain. The afferent signals from the CS produce highly dynamic, adaptive responses to even "simple" stimuli. To better understand the advantageous properties of the system, we constructed a dynamical model that describes some of these adaptive responses. We tuned the model parameters to reproduce the response time-courses from experimental data, and found that the model could describe a variety of additional responses with these same parameter values, suggesting that the model replicates the underlying dynamics of CS afferents without overfitting to the data. In addition, our model captures several gross characteristics of CS responses: 1) Responses encode the magnitude of the applied force; 2) The peak response reflects the rate at which the force is applied; 3) The response adapts to constant applied forces; and 4) The response shows hysteresis under cyclic loading. Improved replication of CS responses to applied forces will enable a more thorough understanding of how the nervous system detects forces and controls walking, and will lead to the development of more robust, self-calibrating strain sensors for robots.

Keywords: Insect, Campaniform Sensilla, Robotics.

1 Introduction

Campaniform sensilla (CS) are sensory organs embedded in the insect cuticle that measure strain [1]. Since stress and strain are related, CS effectively measure the forces acting on the leg. However, CS are not simple sensors. While the sensory discharge (i.e. total afferent nerve firing frequency) does reflect the static level of a constant applied force, the overall response is dominated by sensitivity to force dynamics (e.g. dF/dt) [2, 3]. CS might best be thought of as dynamic sensors whose discharges reflect both force and the rate of force [4] and exhibit hysteresis [2]. CS are also known to be sensitive to the orientation of forces applied to the leg [5, 6].

Sense organs that detect forces are critical for animals to generate adaptive walking

* Supported by the National Science Foundation (Grant Number 1704436)

[7], and similar sensors may also help robots walk. One prominent role that such organs serve for insects is to indicate when a leg is in contact with the substrate by registering forces due to supporting and propelling the body (i.e. during the "stance phase"). This is particularly true for CS on the proximal leg segments [8, 9]. For this reason, we have assembled legged robots in the past that include strain sensors on proximal leg segments that return analog feedback regarding the forces acting on the leg [10, 11]. The robots' neural controllers incorporate this information to assist the transition between the stance phase and swing phase of stepping [12]. Related robots have similar sensor suites [13]. However, the performance of such a controller is sensitive to the precise tuning and calibration of the strain sensors, making them impractical for real-world robotic use. We believe that one reason insects are such adept walkers is that their CS are highly dynamic and adaptive, effectively comparing measurements to their "history" in order to accentuate their sensitivity to changing forces and cancel constant offsets. By more thoroughly understanding CS responses with a dynamic model, we anticipate that we can make our robot sensing more detailed and robust, which may lead to more effective walking control in the future.

The goal of this manuscript is to construct a dynamic model that captures the response of a group of CS when strained in its preferred direction [5, 6]. Previous experimental and modeling work has shown that the CS response is dominated by nonlinear effects, including a transient response that exhibits power law decay instead of exponential decay [14] and frequency-independent phase locking with periodic inputs [15]. These features preclude a linear systems description of CS responses, motivating the nonlinear systems description presented in this manuscript.

Our model's goal is to capture the following features of CS responses: Encode the amplitude of the applied force; reflect the rate of the applied force; adapt to constant applied forces; and exhibit hysteresis to cyclic applied forces. We hypothesize that such features will emerge from a simple dynamic model wherein the sensory response is the sum of three terms: One proportional to the instantaneous input; one that adapts to the current force level via a nonlinear low-pass filter; and a constant offset.

In this manuscript, we describe the collection of CS responses from animal experiments (i.e. "animal data") and the formulation and tuning of our dynamic model of CS responses. We use animal data to select values for our model parameters. We show that the model successfully describes animal data not used in the tuning process, supporting that our model is capturing the fundamental properties of the system. We show that the model can capture several gross features of CS responses, including responses that reflect both the level of force and the rate of force, as well as hysteresis in the response to cyclic loading. Finally, we discuss possible sources for these dynamics, possible implications for how the nervous system must process load, and what advantages these dynamics may offer robots in the future.

2 Methods

2.1 Animal Experimental Methods

Recordings were taken from the tibial CS of the American cockroach (*Periplaneta* *americana*). Activities of axons of the receptors were monitored extracellularly and identified by action potential amplitude and mechanical stimulation/ablation of the cuticular caps [2]. Force waveforms were generated by an analog to digital interface (Spike 2, Cambridge Electronics), applied to the tibia via a probe linked to a DC motor and monitored by strain gauges in the probe [4].

To aid in generating this model, we wished to test CS responses to ramp-and-hold stimuli with different ramp rates but the same hold amplitude. For all stimuli, the hold amplitude was 1.66 mN. The ramp durations tested were 0.125s, 0.224s, 0.456s, and 0.915s. Each ramp-and-hold stimulus was applied to the tibia 11 times. For each stimulus, the duration of the ramp phase was split into 20 bins. The number of spikes that occurred in each bin was counted and used to calculate the mean afferent firing frequency over that bin. Therefore, each "dataset" consisted of a single stimulus described by 20 time points and 20 frequency samples averaged from 11 repetitions of the stimulus. To test the model response to naturalistic stimuli like the animal might experience during walking, force waveforms obtained from freely walking insects were also applied [16].

2.2 Modeling Methods

Modeling Campaniform Sensilla Discharges. We wish to construct a dynamical model that predicts the discharge (i.e. instantaneous firing frequency) of an afferent nerve from a population of campaniform sensilla (CS) given a load stimulus applied in that population's preferred direction [5, 6]. The sensory discharge of such nerves is known to reflect both the amplitude and rate of a load stimulus [2]. In addition, the sensory discharge adapts as a constant force is applied. Therefore, we choose to model the sensory discharge as the sum of three terms: One proportional to the load stimulus; one that adapts to the load over time; and a constant offset. We expect that rate-sensitivity and hysteresis will emerge naturally from adaptation to stimuli.

We are not attempting to model the separate contribution of individual features in the system, for example, the mechanical response of the CS to limb bending, the intrinsic properties of the sensory or afferent neurons, or the processing performed by individual afferents in the nerve. At this stage, we wish to understand the phenomenological relationship between the force applied to an insect's leg and the rate-coded information carried by the afferent nerves from the CS to the rest of the nervous system. We will refer to these elements collectively as "the system." Possible contributions of each component of the system to the response are considered in the Discussion.

Conceptually, an adaptive response can be thought of as subtracting the long-term history of the input from the input value itself. Thus, the response will reflect the input's rapid changes relative to its history, but will eventually return to zero if the input stops changing and the history can "catch up". Under certain assumptions, it can be shown that such a system directly approximates the rate of change of the input [17]. But how should the long-term history of the input be calculated? In the following, we demonstrate how the properties of a low-pass filter inform the correlation between the total response and the rate of change of the input. Then, we show that a power law low-pass filter matches the response of CS.

Let the instantaneous firing frequency of a CS afferent, y, be the difference between the applied force, u, and a low-pass filtered version of the applied force, x, scaled by a constant, a:

$$y = \mathrm{a} \cdot (u - x). \tag{1}$$

Let x be a low-pass filtered copy of u with time constant τ,

$$\tau \cdot \dot{x} = f(u - x), \tag{2}$$

where $f(z)$ is a function such that $f(0) = 0$ and $\frac{df}{dz} \geq 0\ \forall z$. This implies that $f(z) < 0$ if $z < 0$, and that $f(z) > 0$ if $z > 0$. These conditions ensure that the only equilibrium state is $x = u$ and that the inverse function $f^{-1}(z)$ exists [18].

We seek to understand how y reflects $\dot{u}$, the time-rate of change of u. If $x(t) = u(t - \Delta t)$, then Eq. (1) would mimic a finite difference equation and y would be proportional to $\dot{u}$. How do we enforce that $x(t) = u(t - \Delta t)$, and how do we determine Δt? Let us consider the case where u is a ramp function of the form $u = \frac{A}{T} \cdot t$. We assume that the particular solution to Eq. (2) is the same as u, but delayed in time [17]. This implies that $\dot{x} = \dot{u} = \frac{A}{T}$. Plugging this assumption into Eq. (2),

$$\tau \cdot \frac{A}{T} = f\left(\frac{A}{T} \cdot t - x(t)\right). \tag{3}$$

We can solve Eq. (3) for the particular solution of x,

$$x(t) = \frac{A}{T} \cdot \left(t - \frac{T}{A} \cdot f^{-1}\left(\tau \cdot \frac{A}{T}\right)\right). \tag{4}$$

If we define

$$\Delta t = \frac{T}{A} \cdot f^{-1}\left(\tau \cdot \frac{A}{T}\right). \tag{5}$$

Then, x lags u by Δt, where

$$x(t) = u(t - \Delta t). \tag{6}$$

In the special case that $f(z) = z$, $f^{-1}(z) = z$ such that the solution to Eq. (4) becomes $\Delta t = \tau$ and $x = \frac{A}{T} \cdot (t - \tau)$, such that x lags u by a constant amount independent of the value of $\dot{u}$ [17]. However, we are not limited to this particular case. To understand how $f(z)$ impacts y, let us write the finite difference approximation of $\dot{u}$:

$$\Delta t \cdot \dot{u} \approx u(t) - u(t - \Delta t). \tag{7}$$

Substituting Eqs. (5) and (6) into Eq. (7),

$$\frac{T}{A} \cdot f^{-1}\left(\tau \cdot \frac{A}{T}\right) \cdot \dot{u} = u(t) - x(t). \tag{8}$$

Substituting Eq. (8) into Eq. (1), we find that y is proportional to $\dot{u}$ in steady state:

$$y = a \cdot (u - x) = a \cdot \frac{T}{A} \cdot f^{-1}\left(\tau \cdot \frac{A}{T}\right) \cdot \dot{u}. \tag{9}$$

Equation (9) simplifies when we recall that for this example, $\dot{u} = \frac{A}{T}$:

$$y = a \cdot f^{-1}(\tau \cdot \dot{u}). \tag{10}$$

Therefore, $\dot{u}$ maps to y according to the inverse function of the low-pass filter function, $f(z)$. For example, if a system's output follows a logarithmic encoding of the input's rate of change, then $f(z)$ should be an exponential function. The sensory discharge of CS reflect the rate of force according to a power law relationship [2, 3]. Therefore, our model's $f(z)$ should also be a power law with the reciprocal exponent of the power law correlation between $\dot{u}$ and y. However, if the response were modeled only by $f(z)$, then the model could not capture the observed component of the response that is proportional to and offset from the tonic applied force [2]. Thus, we add two such terms.

The model used in this manuscript is as follows:

$$y = \max(0, a \cdot (u - x) + b \cdot u + c), \tag{11}$$

$$\tau \cdot \dot{x} = sign(u - x) \cdot |u - x|^{d}, \tag{12}$$

where y is the instantaneous firing frequency (Hz) of afferent nerves from a population of CS; u is the instantaneous loading (mN) of the limb segment in the CS population's preferred orientation; x is a low-pass filtered copy of u; a scales the adaptation term $u - x$; b is the proportionality constant between u and y; c is a constant offset; d is the power law exponent that describes the low-pass filter function $f(z)$; and τ is a time scaling factor for $\dot{x}$. To avoid the introduction of imaginary numbers, Eq. (12) raises the absolute value of the argument, $u - x$, to the power of d, and then multiplies by the sign of the argument. In total, this model requires that five numerical parameters be tuned $(a, b, c, d,$ and $\tau)$.

Tuning Model Parameters. Model parameters were tuned via optimization. Gradient-based optimization (fmincon, Matlab, The Mathworks, Natick, MA) set the model parameter values to minimize the difference between the model's response time-course and the smoothed CS firing frequency response time-course given the same applied force. For each parameter value configuration tested, an applied force was specified and the model's response was simulated. The root-mean-squared error between the simulation output and the corresponding CS firing frequency response was returned as the objective to minimize. To test that the model could capture the underlying dynamics of the system and generalize to other cases, only two experimental time-courses (the fastest and the slowest) were used to tune the system. By selecting the most extreme stimuli, we test our model's ability to interpolate the dynamic response of the CS in response to intermediate stimuli.

3 Results

3.1 Model Tuning and Generalization

To avoid overfitting model parameters, we used two experimental datasets to tune model parameters, and then observed the goodness of fit to additional experimental datasets. Figure 1 shows four plots, each depicting the force input, the response from the corresponding animal dataset, and the response from the model. The two trials on the left were used to tune the parameter values, which are listed in Table *1*. The two trials on the right show animal and model responses to additional stimuli, but these trials were not used to tune the parameters. Remarkably, the model responses on the right capture the dynamic nature of the animal responses despite not being tuned to do so. This suggests that the model captures the underlying dynamics of the system.

Recent studies on stick insects have demonstrated that CS responses to force stimuli like those the animal would generate during locomotion are more dynamic and adapt less quickly than responses to conventional stimuli (i.e. ramp-and-hold stimuli) [4]. We

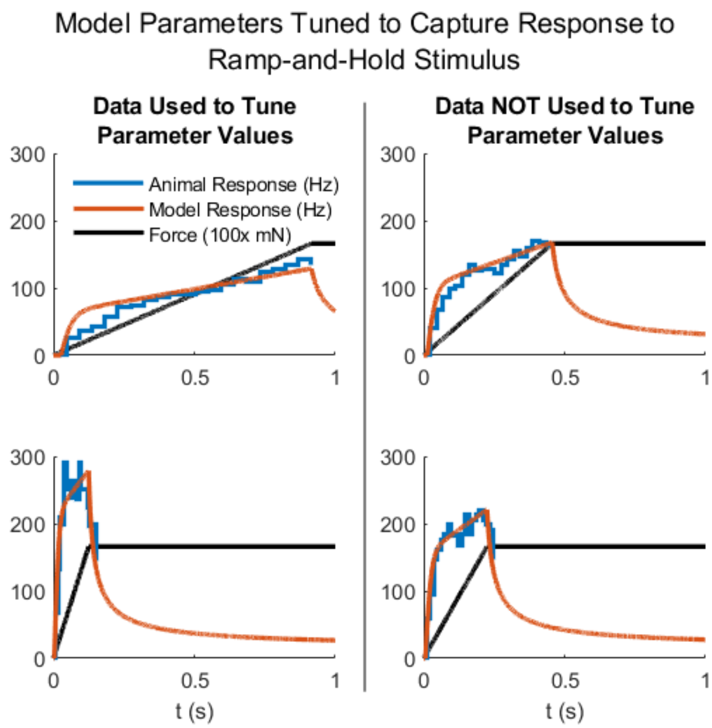

Figure 1 – Animal data were used to tune the constant parameters of the model. Left: Two datasets were used to select values for the parameters a, b, c, d, and τ that reduced the mean-squared-error between the animal response and the model response, given the same input force. Right: The model captures these other animal responses remarkably well, despite not explicitly being tuned to match.

Table 1 – Model parameter descriptions and values.

Parameter	Description	Value
a	Adaptation term scale	1088
b	Proportional term scale	40.45
c	Constant offset	-52.84
d	Exponent in low-pass filter function, i.e. $f(z) = z^d$	2.369
τ	Time constant for $\dot{x}$	2.668×10^3

wished to see if the model could capture the same characteristics without retuning the model parameters. Figure *2* shows the model's response to both a ramp-and-hold stimulus and to a naturalistic stimulus. Figure *2*A shows that the responses to the ramp-and-hold stimulus share several key characteristics: Both responses initially leap up to a high value; both responses then continue to grow, but at a reduced and apparently constant rate; both responses quickly adapt during the hold portion of the stimulus; both responses are quickly eliminated during the downward ramp. The peak response of the experimentally measured CS response is 25-30 Hz higher than that of the model. However, the shape of both the rising phase and the relaxation phase qualitatively match, suggesting that the model is capturing the underlying dynamics of the system. In addition, the adaptation phases largely overlap, despite the model being tuned without any data from the relaxation phase.

Figure *2*B also shows that the responses to the naturalistic stimulus largely match between the model and the animal, despite the dynamic nature of the stimulus and not retuning the parameter values. The responses share several key characteristics: Both responses are sensitive to the initial increase in the force; both responses are largely constant between 10% and 40% of the stimulus duration, despite the dynamic nature of the force's rise; both responses slowly adapt, and then are silenced when the force noticeably decreases at around 80% of the stimulus.

Figure *2*C compares the model's response to the two stimuli. As seen in the experimentally measured CS responses, the response to the ramp-and-hold stimulus increases more rapidly, reaches a higher response frequency, and adapts more quickly than the response to the naturalistic stimulus. The response to the naturalistic stimulus is persistent despite the dynamic nature of both the force stimulus and the model. These data suggest that the CS are tuned to detect relevant sensory features during walking [4].

3.2 Emergent Properties of the Model

Our model reproduces the linear encoding of tonic force levels as well as the power law reflection of the rate of force seen in insect CS [2]. Figure *3* shows data summarizing simulation experiments in which the model was subjected to a ramp-and-hold stimulus with a height A and a rise time T (i.e. $u(t) = \min(A \cdot t/T, A)$). Figure *3*A shows that as in the animal, the sensory discharge long after the hold phase begins (in our experiments, 9.5 seconds in accordance with [2]) is linearly correlated with the amplitude of the force, A.

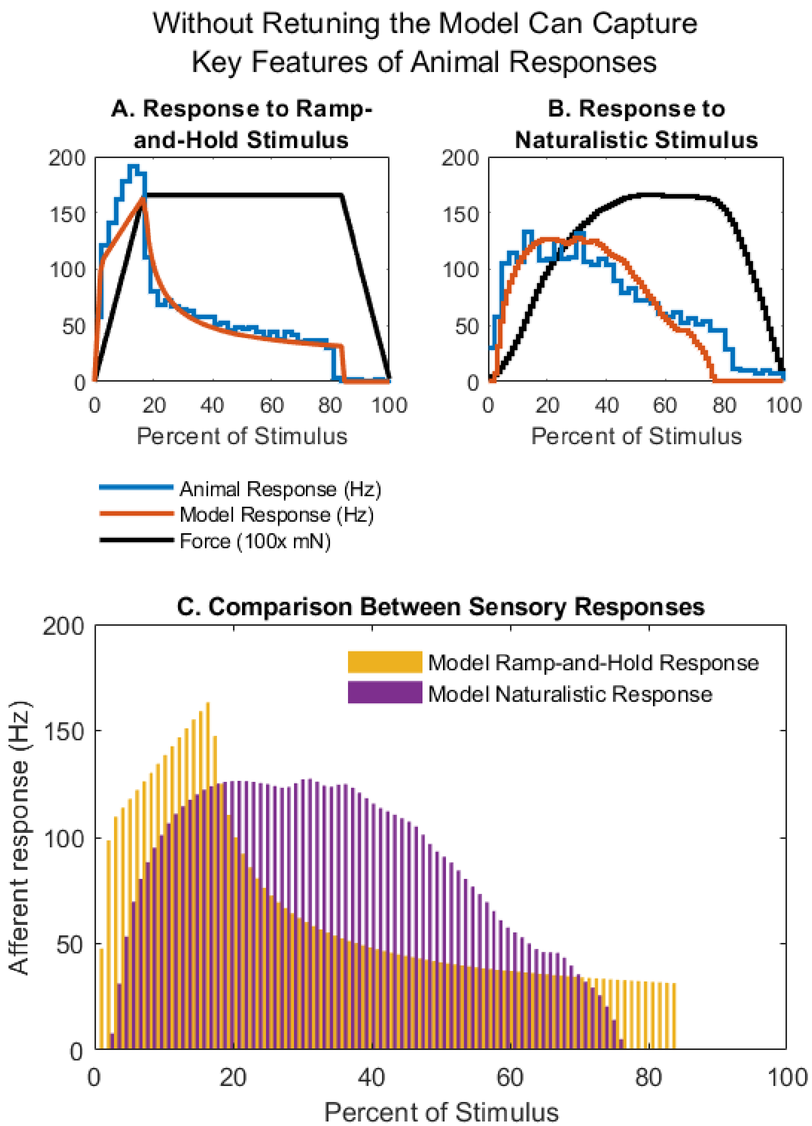

Figure 2 – The differences between the model's response to ramp-and-hold and naturalistic stimuli reflect those seen in the animal. A) Using the original model tuning, the model captures the animal response to both the ramp and hold portions of the stimulus. The model has not been tuned to capture the hold phase data. B) The model response to an animal-like force waveform resembles the animal response to the same stimulus, despite not being tuned to do so. C. As seen in the animal data, the model response to the ramp-and-hold stimulus peaks higher and adapts more quickly than the response to the naturalistic stimulus. This suggests a fundamental similarity between the model and the animal.

Our model response reflects the rate of force despite no explicit dependence on it. Figure *3*B shows that as in the animal, the maximum sensory discharge reflects the rate

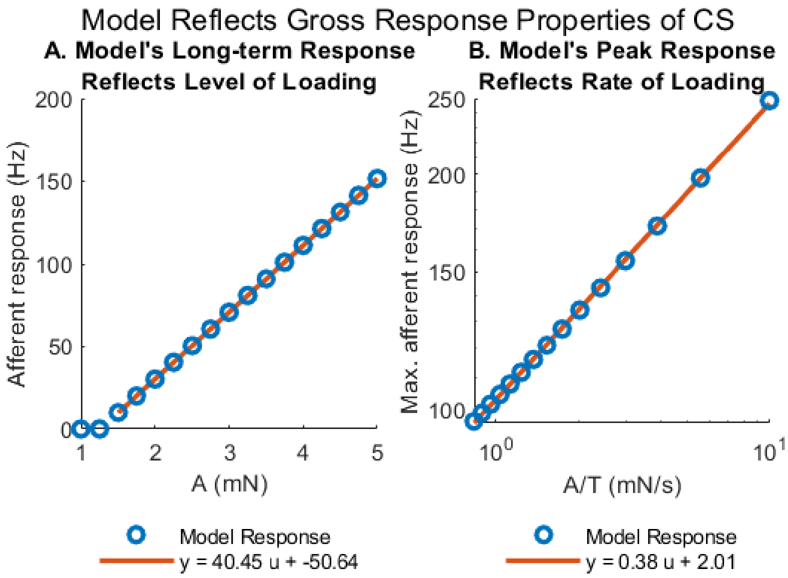

Figure 3 – The model shares the same gross response properties as animal CS. A) The model response linearly encodes the applied force amplitude A, 10 seconds after the stimulus is applied (ramp duration of 0.5 seconds). B) The model's peak response reflects the rate of loading $\frac{A}{T}$ via a power law relationship. Note the logarithmic axes. The slope of the line of best fit represents the exponent of the power law relationship. A value of 0.35 is consistent with previous characterizations of cockroach proximal tibial CS responses [2].

of loading, A/T. Note that both the horizontal and vertical axes are logarithmically scaled, such that this apparently linear correlation is actually a power law correlation. The calculated slope is precisely in agreement with previous characterizations of cockroach proximal tibia CS, and is also roughly what would be expected based on our model tuning (i.e. $d^{-1} = 0.422$, compare to values in Table 1 in [2]). Also note that the response to the rate of loading is substantially higher than the response to the amplitude of the load. This is consistent with CS being fundamentally dynamic sensors [4].

Our model response exhibits hysteresis in response to loading and unloading as seen in insect CS [2]. Figure *4* shows data from a simulation experiment in which the model was subjected to a “staircase” stimulus, in which the applied force was stepped up and then stepped down at the same levels. The response in Figure *4*A shows large fluctuations due to adaptation, in which the response is strongly biased in the direction of the change in force. Figure *4*B shows the form of the “staircase” stimulus. Figure *4*C plots the mean sensory response during the tonic segments of the staircase. The color coding matches that in Figure *4*A, to impress a sense of time. The model's response to a given force depends on the history of the sensory input, that is, whether the force was increased or decreased to that level.

4 Discussion

In this manuscript, we assembled a dynamic model of the sensory discharges observed from afferent nerves from insect campaniform sensilla (CS). CS discharges are proportional to the bending forces applied to the leg, but also demonstrate strong adaptive responses and hysteresis. Additionally, such adaptation does not match the output of a linear model [14], so we derived a method for designing a nonlinear low-pass filter that can replicate the response properties of CS afferent nerves. We then subjected this model to stimuli like those applied to insect legs and used some experimental data to tune the constants in the model. Once complete, the model could capture the results of experiments whose data were not used to tune the model, including the response to highly dynamic inputs. In addition, the model exhibited the same gross responses seen in the animal: Linear encoding of the applied force level; power law reflection of the rate of the applied force; and hysteresis in response to cyclic loading.

The model we developed is only a phenomenological model, but may have benefits for experimental neuroscience and robotics. With a phenomenological description of CS response to a given force input, experimental stimuli can be derived that may produce more natural CS responses. For example, previous studies have shown that the

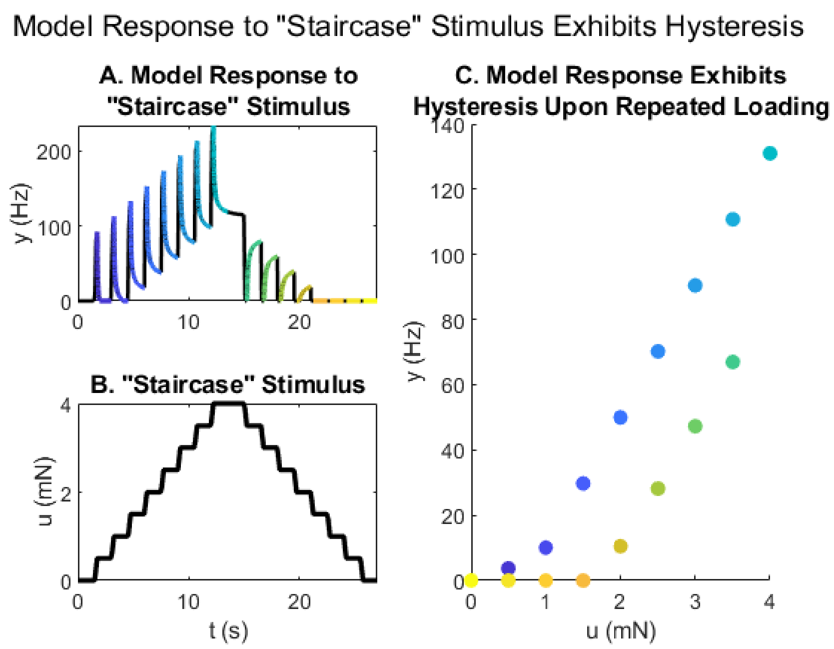

Figure 4 – As observed in the animal, the model response exhibits hysteresis. A) The response to a “staircase” stimulus shows the strong history dependence of the response; specifically, the response is biased in the direction of the rate of change of the force. B) The “staircase” stimulus. C) The mean model responses during the hold phases of the “staircase” reveal a clear hysteresis loop upon cyclic loading. The points are calculated as the mean response y while u is not changing. The color coding relates to the traces in A).

history of loading has discrete effects upon CS encoding, specifically, that pre-loading the leg resets the amplitude sensitivity, while dynamic properties (e.g. encoding the rate of change of force) are not altered by history [2]. Conversely, the model could be inverted to infer the instantaneous force acting on a leg given the CS recording during motion. Using animal kinematic and force measurements to build a model of insect walking has already led to a better understanding of the types of forces these sensors are subjected to as the animal walks freely [16]. Better understanding the responses to these forces will elucidate what information the nervous system has available to it regarding forces applied to its legs.

This model will also benefit robotics. To better understand how the insect nervous system uses CS feedback in the control of walking, we have built such strain sensors into the legs of our robots [10, 11]. Such sensors are particularly useful for detecting when a leg is in the "stance phase," during which it supports and propels the body, versus when it is in the "swing phase." In the past, these sensors have provided our stepping controllers with non-adapting feedback proportional to the force on the leg. However, calibrating such sensors to eliminate constant offsets while maintaining maximal sensitivity is critical for proper function; if the offset is too high, the sensors return false-positive information about leg loading; if the offset is too low, the sensors return false-negative information. We believe that our CS response model could be implemented to run in real-time onboard robots, enabling their sensors to self-calibrate. Such an algorithm would adapt to cancel out offsets, but remain sensitive to sudden changes in the force level (e.g. from a leg transitioning from the swing phase to the stance phase). Such self-calibration may increase the reliability of large arrays of analog sensors onboard robots that provide feedback regarding support and contact forces, environmental fluid currents (e.g. via hairs), and other body-wide conditions.

What specific structures might give rise to the dynamics we describe in this manuscript? Experimental data and computational modeling of spider mechanoreceptors suggest that adaptation arises due to adaptive ion channels present in receptor cells [19]. The viscoelastic hysteresis of the exoskeleton and the CS themselves is also known to contribute to sensory adaptation [20]. Future experiments may reveal additional sources of adaptation. Better understanding such sources may suggest new sensor designs or processing algorithms that would endow walking robots with animal-like mobility.

References

1. Zill, S.N., Schmitz, J., Büschges, A.: Load sensing and control of posture and locomotion. Arthropod Struct. Dev. 33, 273–86 (2004).
2. Ridgel, A.L., Frazier, S.F., DiCaprio, R.A., Zill, S.N.: Encoding of forces by cockroach tibial campaniform sensilla: implications in dynamic control of posture and locomotion. J. Comp. Physiol. A Sensory, Neural, Behav. Physiol. 186, 359–374 (2000).
3. Zill, S.N., Büschges, A., Schmitz, J.: Encoding of force increases and decreases by tibial campaniform sensilla in the stick insect, Carausius morosus. J. Comp. Physiol. A Neuroethol. Sensory, Neural, Behav. Physiol. 197, 851–867 (2011).
4. Zill, S.N., Dallmann, C.J., Büschges, A., Chaudhry, S., Schmitz, J.: Force dynamics and

synergist muscle activation in stick insects: the effects of using joint torques as mechanical stimuli. J. Neurophysiol. 120, 1807–1823 (2018).

5. Zill, S.N., Moran, D.T.: The Exoskeleton and Insect Proprioception. I. Responses of Tibial Campaniform Sensilla to External and Muscle-Generated Forces in the American Cockroach, Periplaneta Americana. J. Exp. Biol. 91, 1–24 (1981).
6. Zill, S.N., Schmitz, J., Chaudhry, S., Büschges, A.: Force encoding in stick insect legs delineates a reference frame for motor control. J. Neurophysiol. 108, 1453–72 (2012).
7. Ekeberg, Ö., Blümel, M., Büschges, A.: Dynamic simulation of insect walking. Arthropod Struct. Dev. 33, 287–300 (2004).
8. Noah, J.A., Quimby, L., Frazier, S.F., Zill, S.N.: Walking on a “peg leg”: Extensor muscle activities and sensory feedback after distal leg denervation in cockroaches. J. Comp. Physiol. A Neuroethol. Sensory, Neural, Behav. Physiol. 190, 217–231 (2004).
9. Akay, T., Bässler, U., Gerharz, P., Büschges, A.: The Role of Sensory Signals From the Insect Coxa-Trochanteral Joint in Controlling Motor Activity of the Femur-Tibia Joint. J. Neurophysiol. 85, 594–604 (2001).
10. Szczecinski, N.S., Chrzanowski, D.M., Cofer, D.W., Terrasi, A.S., Moore, D.R., Martin, J.P., Ritzmann, R.E., Quinn, R.D.: Introducing MantisBot: Hexapod robot controlled by a high-fidelity, real-time neural simulation. In: IEEE International Conference on Intelligent Robots and Systems. pp. 3875–3881. , Hamburg, DE (2015).
11. Goldsmith, C., Szczecinski, N.S., Quinn, R.D.: Neurodynamic modeling of the Fruit Fly Drosophila melanogaster. Bioinspir. Biomim. (2020).
12. Szczecinski, N.S., Getsy, A.P., Martin, J.P., Ritzmann, R.E., Quinn, R.D.: MantisBot is a Robotic Model of Visually Guided Motion in the Praying Mantis. Arthropod Struct. Dev. (2017).
13. Schäffersmann, M., Schneider, A., Schmitz, J.: Self-adjustable transducer for bio-inspired strain detection in walking legs. In: Mobile Service Robotics. pp. 199–206. World Scientific (2014).
14. Chapman, K.M., Smith, R.S.: A linear transfer function underlying impulse frequency modulation in a cockroach mechanoreceptor. Nature. 197, 699–700 (1963).
15. French, A.S., Holden, A. V., Stein, R.B.: The estimation of the frequency response function of a mechanoreceptor. Kybernetik. 11, 15–23 (1972).
16. Dallmann, C.J., Dürr, V., Schmitz, J.: Joint torques in a freely walking insect reveal distinct functions of leg joints in propulsion and posture control. Proc. Biol. Sci. 283, 20151708- (2016).
17. Szczecinski, N.S., Hunt, A.J., Quinn, R.D.: A functional subnetwork approach to designing synthetic nervous systems that control legged robot locomotion. Front. Neurorobot. 11, (2017).
18. Khalil, H.K.: Nonlinear Systems. Prentice Hall (2002).
19. French, A.S., Torkkeli, P.H.: The power law of sensory adaptation: Simulation by a model of excitability in spider mechanoreceptor neurons. Ann. Biomed. Eng. 36, 153–161 (2008).
20. Chapman, K.M., Mosinger, J.L., Duckrow, R.B.: The role of distributed viscoelastic coupling in sensory adaptation in an insect mechanoreceptor. J. Comp. Physiol. A. 131, 1–12 (1979).